Electronic Supplementary Material (ESI) for Energy & Environmental Science.

Supplementary Information

Metal-Organic Framework Route to In-Situ Encapsulation of Co@Co_3O_4@C Core@Bishell Nanoparticles into Highly Ordered Porous Carbon Matrix for Oxygen Reduction

Wei Xia, Ruqiang Zou, Li An, Dingguo Xia, and Shaojun Guo**

W. Xia, L. An, Prof. D. G. Xia, Prof. R. Q. Zou
College of Engineering, Peking University, Beijing 100871 (China)
E-mail: rzou@pku.edu.cn

Prof. S. J. Guo
Physical Chemistry and Applied Spectroscopy, Los Alamos National Laboratory, Los Alamos, NM 87545 (USA)
E-mail:shaojun.guo.nano@gmail.com

Figures

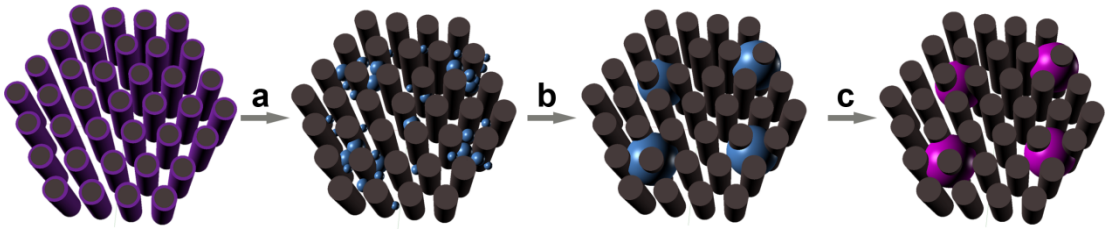

Fig. S1 Schematic illustration of the formation of $Co@Co_3O_4@C$-CM from MOF-CM. (Step a) Small Co nanoparticles (NPs) formed into the pores at high temperature at the initial state. (Step b) As the heat treatment proceeded, small NPs aggregated to form larger Co@C NPs. (Step c) The Co NPs were oxidized to $Co@Co_3O_4$ core@shell NPs after further oxidation process.

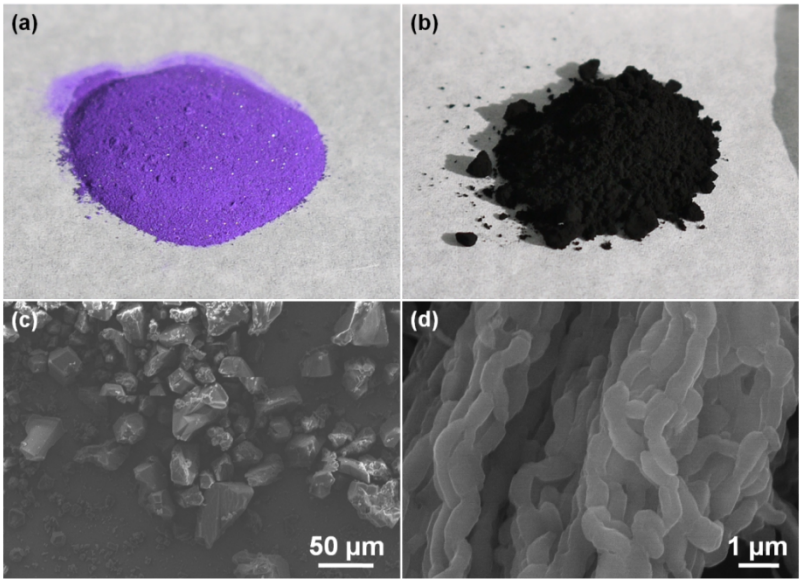

Fig.S2 (a, b) Photographs and (c, d) SEM images of (a, c) MOF and (b, d) CM, respectively.

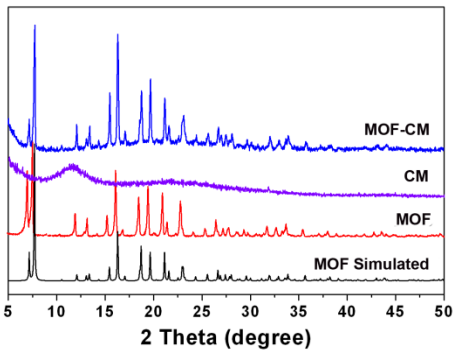

Fig. S3 PXRD patterns of the as-prepared MOF, CM and MOF-CM composite. The simulated PXRD pattern of MOF is listed for reference.

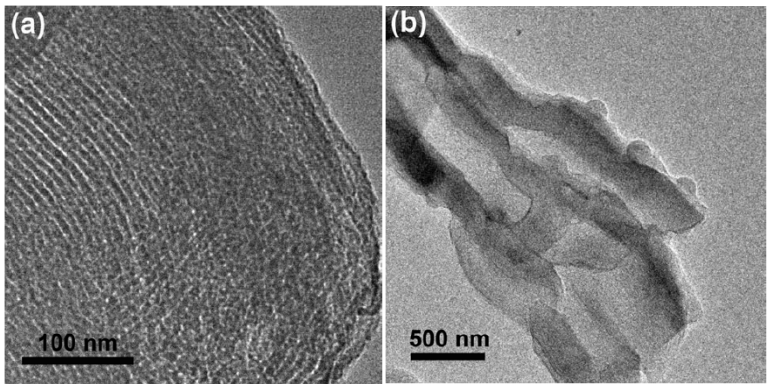

Fig. S4 TEM images of (a) CM and (b) MOF-CM composite.

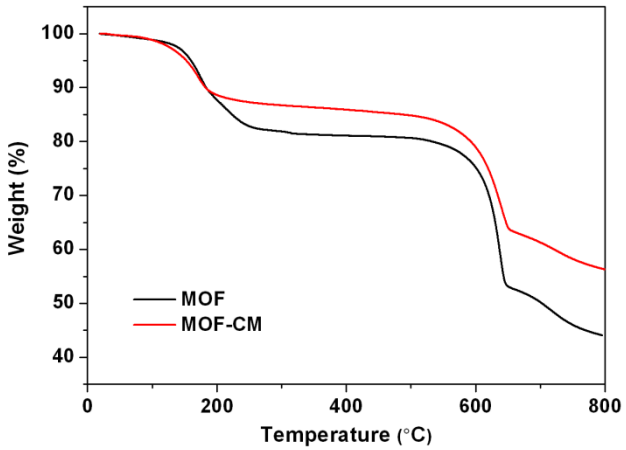

Fig. S5 TG curves of MOF and MOF-CM composite in N_2.

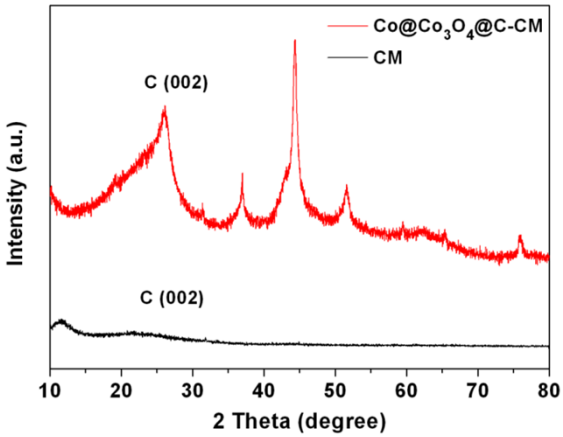

Fig. S6 PXRD patterns of $Co@Co_3O_4@C$-CM and CM. $Co@Co_3O_4@C$-CM has the much higher and sharper C (002) peak than CM.

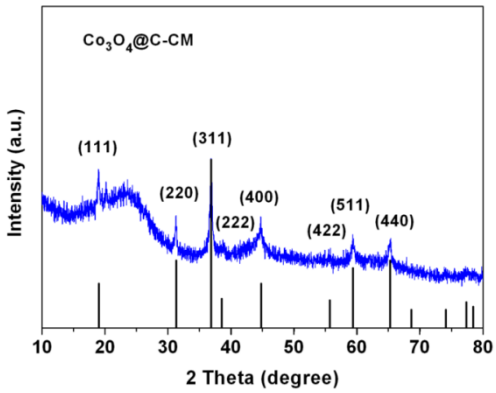

Fig.S7 PXRD pattern of Co_3O_4@C-CM (PDF#42-1467).

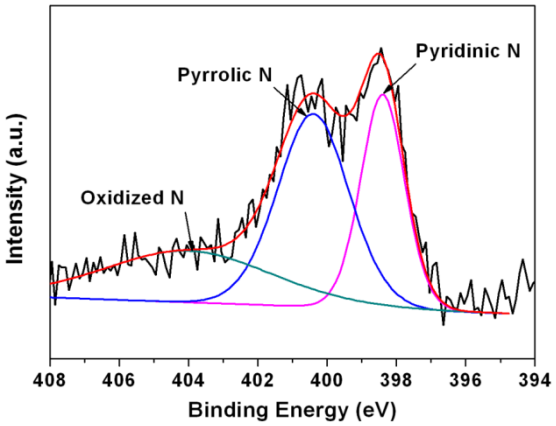

Fig. S8 High-resolution N 1s spectrum of Co@Co_3O_4@C-CM composite.

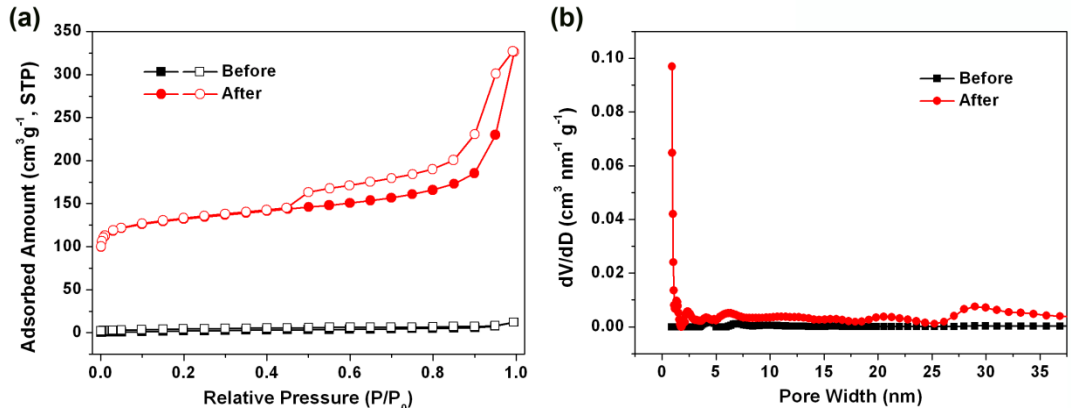

Fig. S9 (a) Nitrogen sorption isotherms and (b) pore size distributions of the pure MOF before and after the same heat treatment and oxidation process. The treatment conditions were similar to that of preparing Co@Co_3O_4@C-CM.

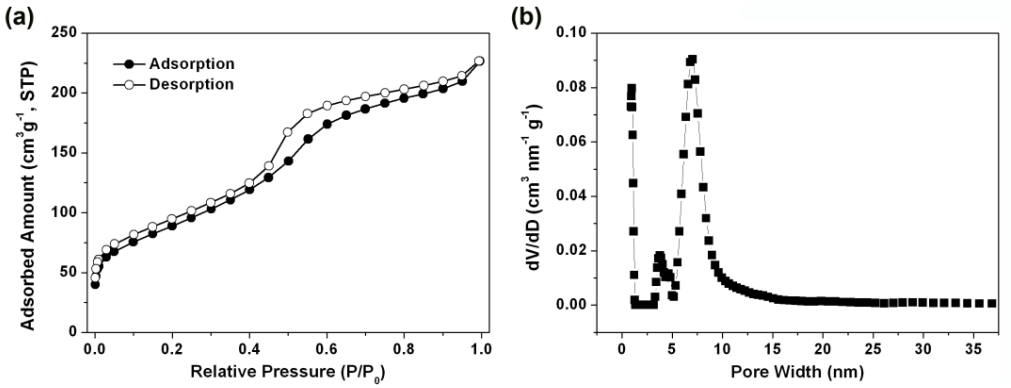

Fig. S10 (a) Nitrogen sorption isotherms and (b) the corresponding pore size distribution of MOF-CM composite.

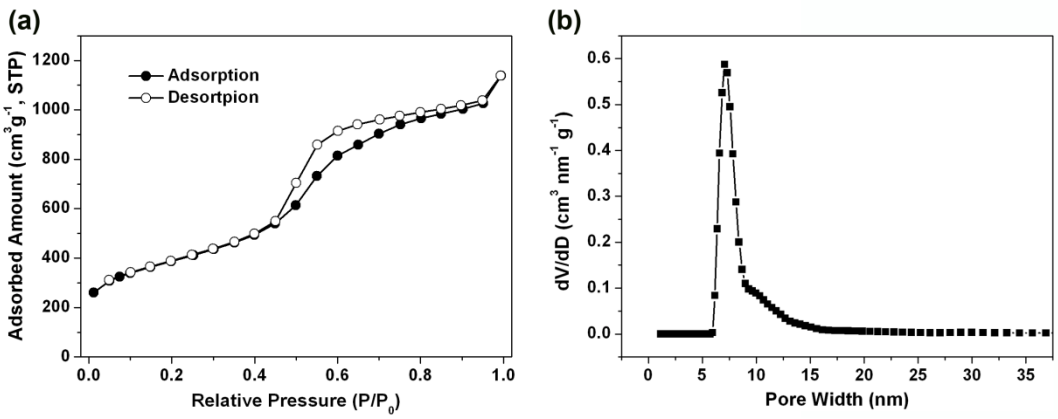

Fig. S11 (a) Nitrogen sorption isotherms and (b) the corresponding pore size distribution of CM. The treatment conditions were similar to that of preparing Co@Co_3O_4@C-CM.

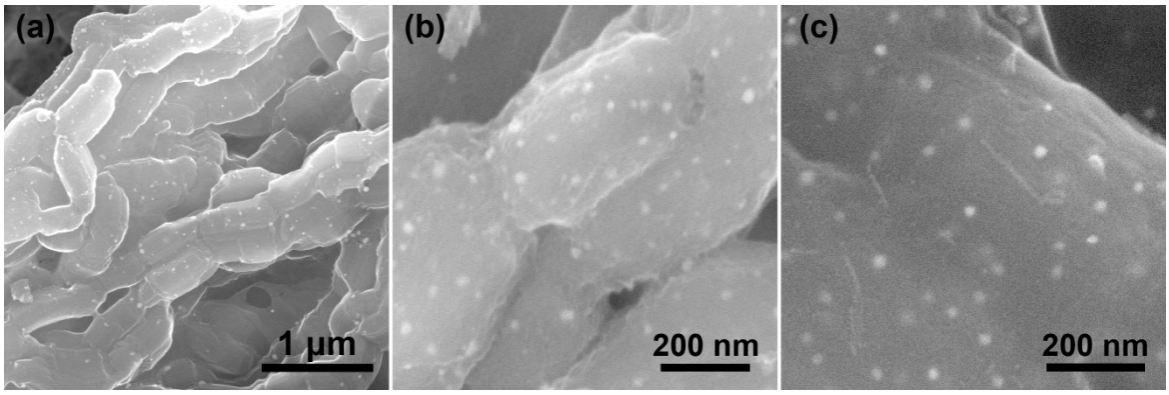

Fig. S12 SEM images of Co@Co_3O_4@C-CM.

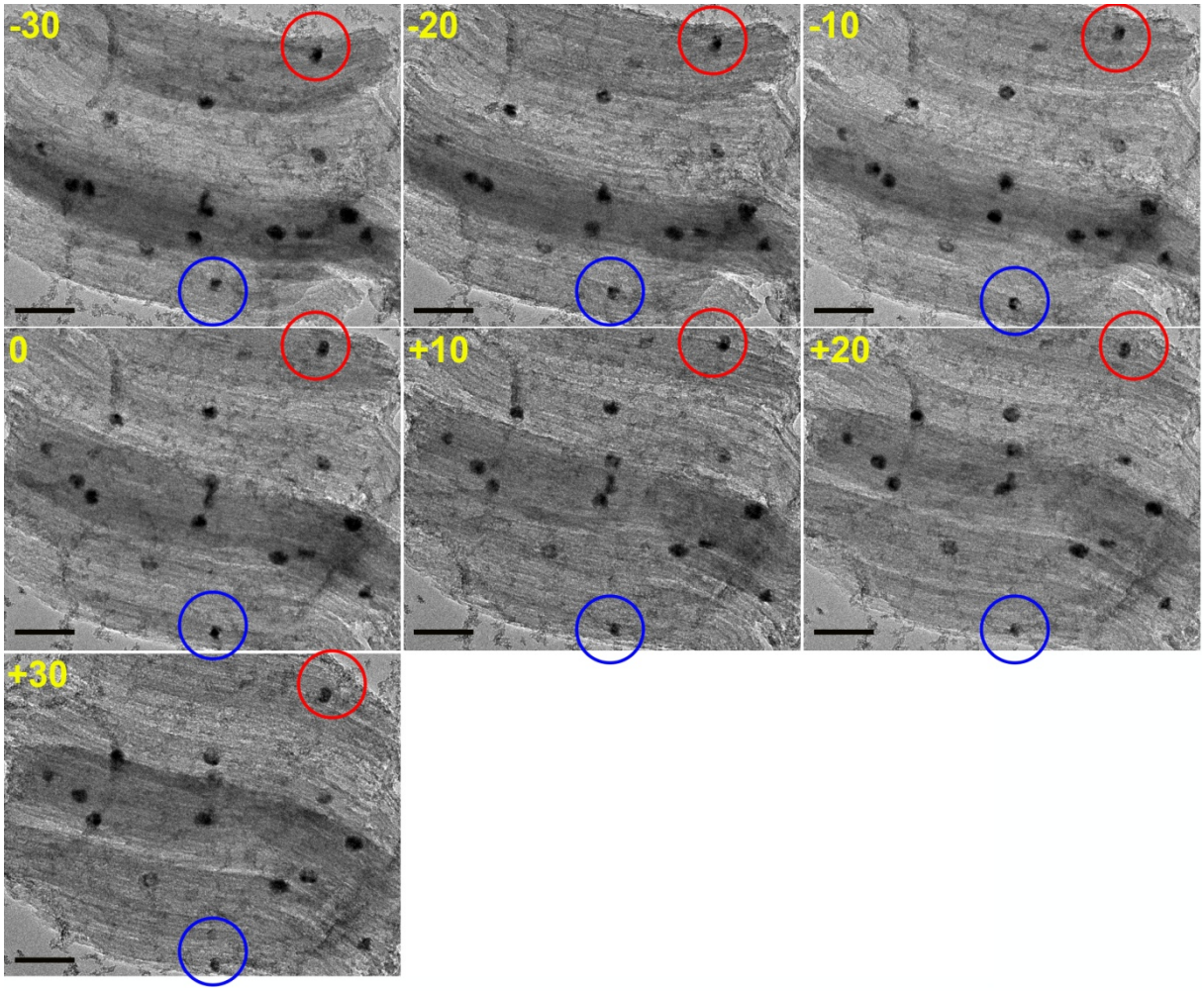

Fig. S13 Images from TEM tilting experiments of $Co@Co_3O_4@C$-CM (scale bar: 100 nm). The sample was rotated from -30° to +30°.

We further used TEM tilting experiments to confirm that the $Co@Co_3O_4@C$ NPs stayed both inside and on the external walls of the CM particle. As shown in **Fig. S13**, the sample was rotated for angles from -30° to +30°. Two NPs were selected for the comparison (marked by red and blue circles). These two NPs are close to the surface of a CM domain. If the NPs locate on the external surface of the CM domain, they will be moved to the edge of the domain from TEM image by rotating. Results showed that the NP marked by blue circle moved outward steady from -30° to +30° and came to the edge of the CM domain at +30°, meaning that it was on the external surface of CM. In comparison, the NP marked by red circle moved slightly outward from -30° to 0° and inward from 0° to +30°. During all the process, it remained inside the domain and did not reach the edge, demonstrating that it located inside CM.

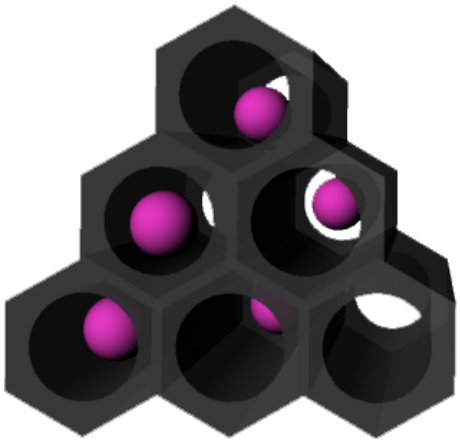

Fig. S14 Structure model of NPs in SBA-15.

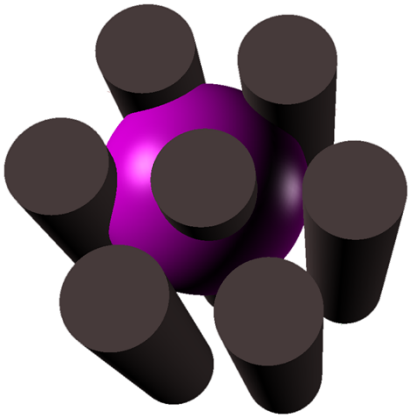

Fig. S15 Structure model of $Co@Co_3O_4@C$-CM.

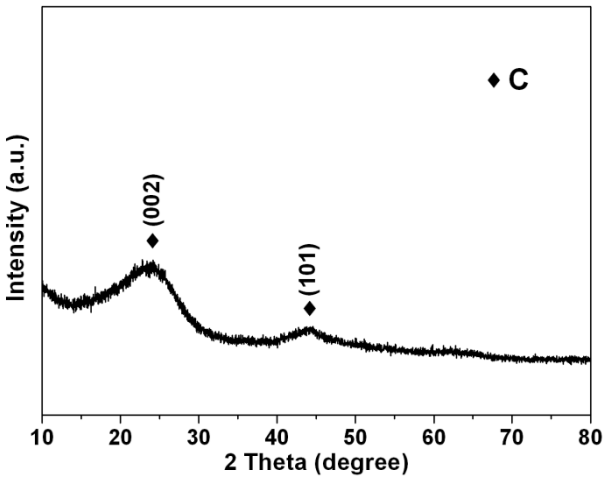

Fig. S16 PXRD pattern of C-CM.

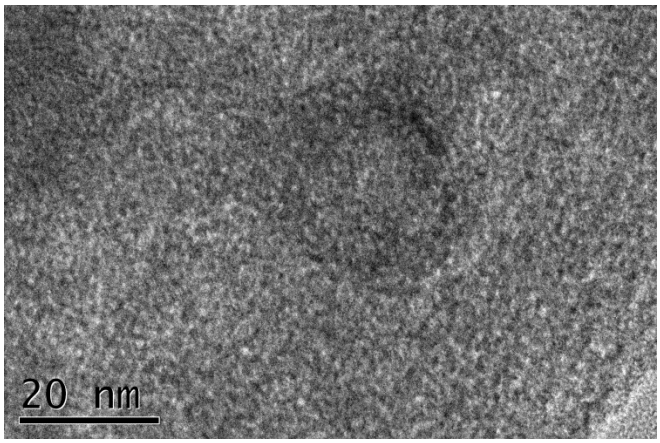

Fig. S17 TEM image of C-CM.

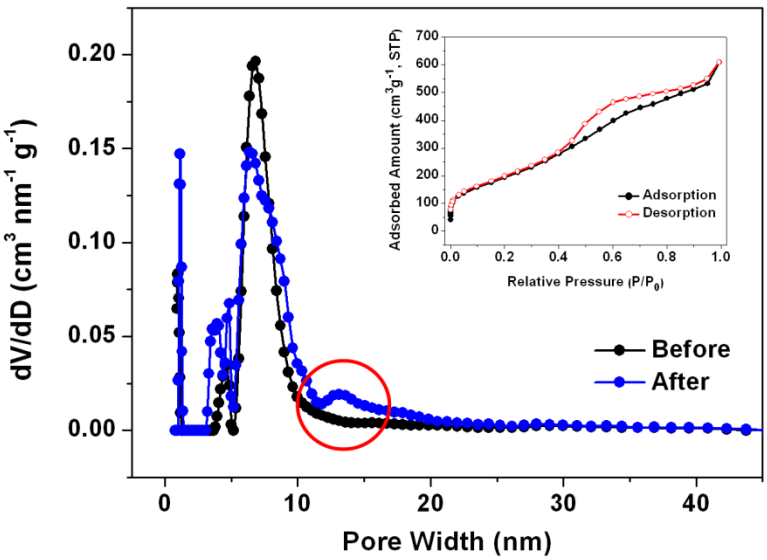

Fig. S18 Pore size distributions of the Co@Co_3O_4@C-CM sample before and after acid wash. Inset shows the nitrogen sorption isotherms of the sample after acid wash.

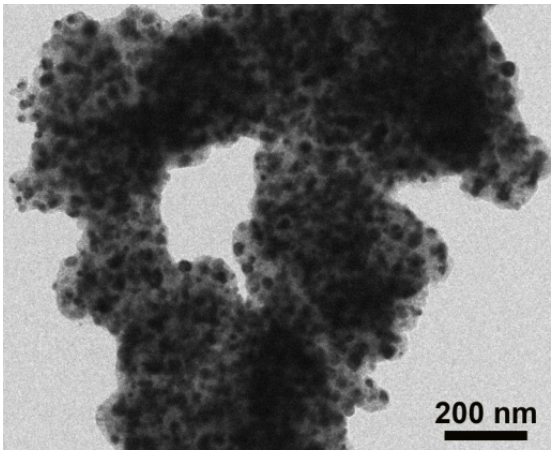

Fig. S19 TEM image of Co@Co_3O_4-C.

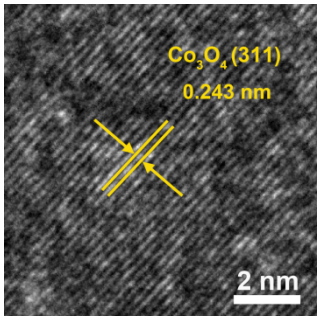

Fig. S20 HRTEM image of Co_3O_4@C-CM.

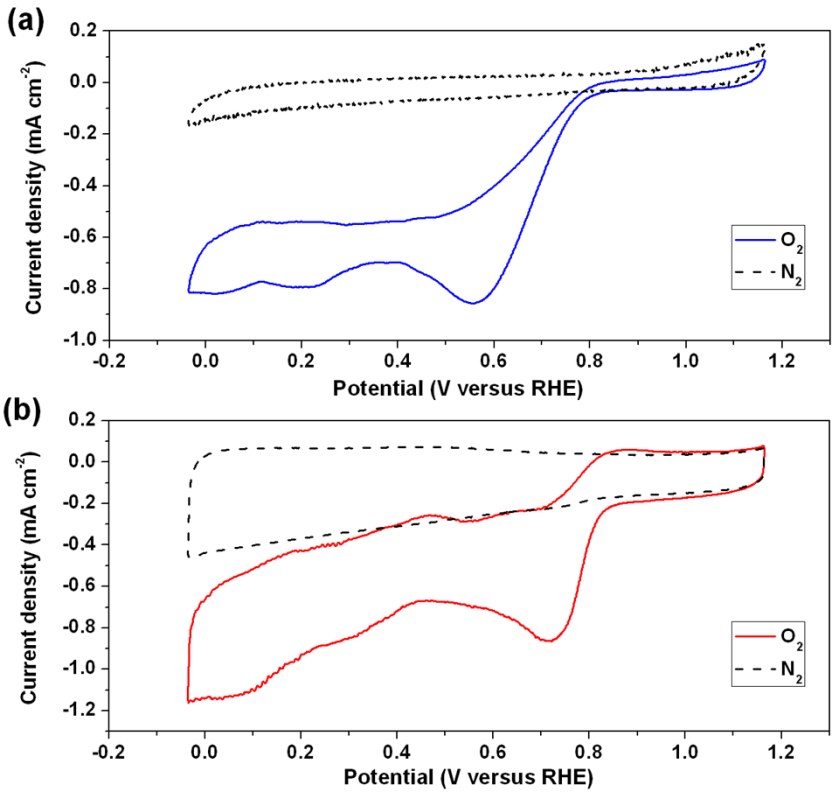

Fig. S21 CVs of CM (a) and Co@Co_3O_4-C (b) in O_2-saturated or N_2-saturated 0.1 M KOH at scanning rate of 50 mV s^{-1}.

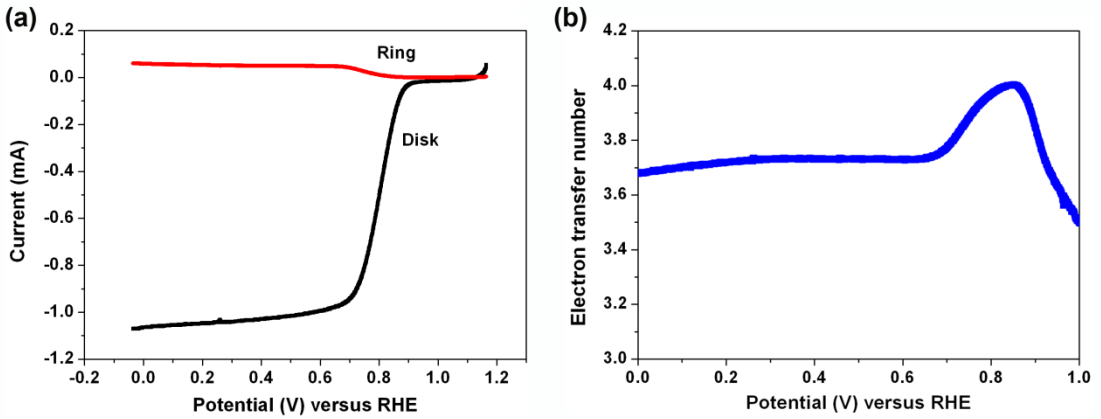

Fig. S22 (a) RRDE curve of Co@Co_3O_4@C-CM at 1600 rpm. (b) Electron transfer number at various potential.

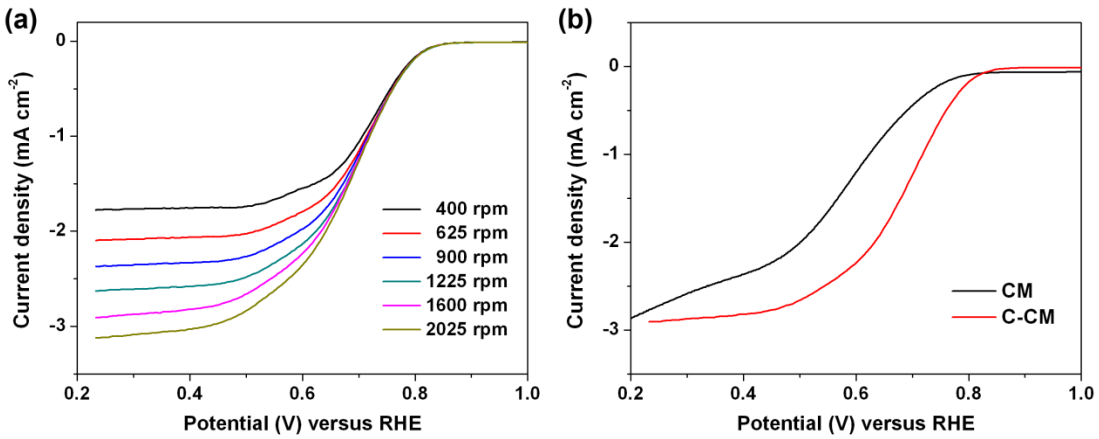

Fig. S23 (a) ORR polarization curves of C-CM at various rotating rate (scan rate: 10 mV s^{-1}). (b) ORR polarization curves of CM and C-CM (scan rate: 10 mV s^{-1}; rotation rate: 1600 rpm).

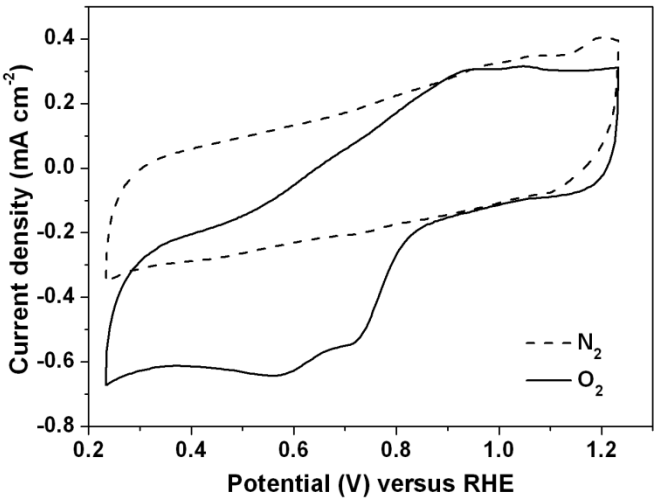

Fig. S24 CVs of Co@Co_3O_4-CM at the scan rate of 50 mV s^{-1}.

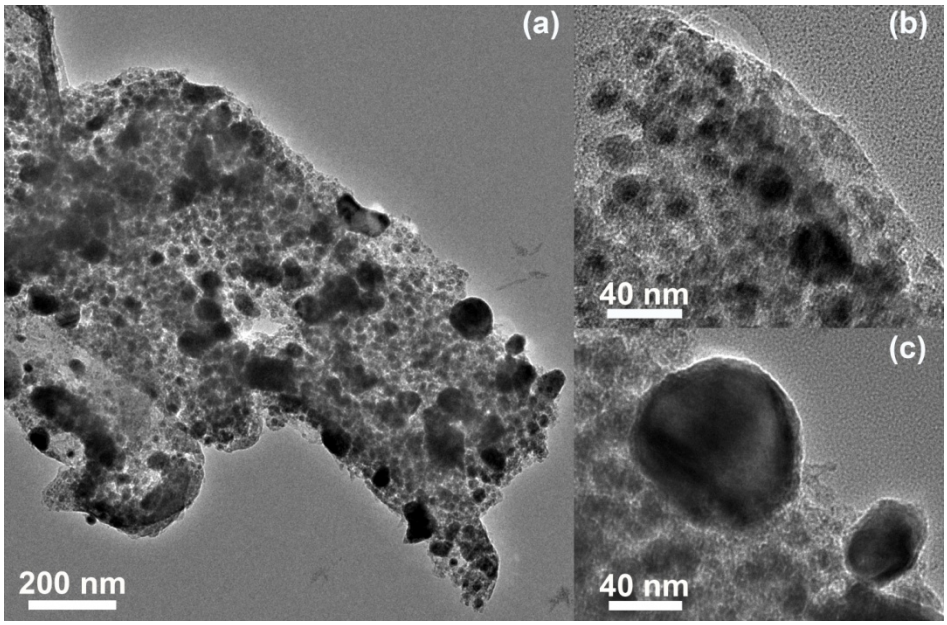

Fig. S25 TEM images of $Co@Co_3O_4$-CM prepared *via* a conventional wet-impregnation method.

Table S1. Summary of the texture parameters of the as-prepared samples.

Sample	S_{BET}[a] (m^2 g^{-1})	D[b] (nm)	V[c] (cm^3 g^{-1})
MOF	9	4.52	0.02
CM	1340	7.07	1.76
MOF-CM	313	7.07	0.35
$Co@Co_3O_4$-C	466	0.93	0.50
$Co@Co_3O_4$@C-CM	616	6.83	0.74

[a] S_{BET}: specific surface area from BET method. [b] D: pore diameter from QSDFT (adsorption branch, slit/cylinder/sphere pores model). [c] V: pore volume at relative pressure $P/P_0 = 0.995$.